Visual Neuroscience (2001), **18**, 501–516. Printed in the USA.

DOI: 10.1017.S0952523801184014

Motion direction signals in the primary visual cortex of cat and monkey

WILSON S. GEISLER, DUANE G. ALBRECHT, ALISON M. CRANE, AND LAWRENCE STERN

Department of Psychology and Center for Vision and Image Sciences, University of Texas, Austin

(Received July 27, 2000; Accepted March 28, 2001)

Abstract

When an image feature moves with sufficient speed it should become smeared across space, due to temporal integration in the visual system, effectively creating a spatial motion pattern that is oriented in the direction of the motion. Recent psychophysical evidence shows that such "motion streak signals" exist in the human visual system. In this study, we report neurophysiological evidence that these motion streak signals also exist in the primary visual cortex of cat and monkey. Single neuron responses were recorded for two kinds of moving stimuli: single spots presented at different velocities and drifting plaid patterns presented at different spatial and temporal frequencies. Measurements were made for motion perpendicular to the spatial orientation of the receptive field ("perpendicular motion") and for motion parallel to the spatial orientation of the receptive field ("parallel motion"). For moving spot stimuli, as the speed increases, the ratio of the responses to parallel *versus* perpendicular motion increases, and above some critical speed, the response to parallel motion exceeds the response to perpendicular motion. For moving plaid patterns, the average temporal tuning function is approximately the same for both parallel motion and perpendicular motion; in contrast, the spatial tuning function is quite different for parallel motion and perpendicular motion (band pass for the former and low pass for the latter). In general, the responses to spots and plaids are consistent with the conventional model of cortical neurons with one rather surprising exception: Many cortical neurons appear to be direction selective for parallel motion. We propose a simple explanation for "parallel motion direction selectivity" and discuss its implications for the motion streak hypothesis. Taken as a whole, we find that the measured response properties of cortical neurons to moving spot and plaid patterns agree with the recent psychophysics and support the hypothesis that motion streak signals are present in V1.

Keywords: Visual cortex, Receptive fields, Motion, Direction Selectivity

Introduction

A central question in perception research is how the visual system determines the direction of object motion. The most widely held view is that velocity components are measured at two or more spatial orientations and then combined in some fashion, such as with the "intersection of constraints rule" (see for example, Marr & Ullman, 1981; Adelson & Movshon, 1982; Albright, 1984; Watson & Ahumada, 1985; Stone et al., 1990; Derrington & Suero, 1991; Smith & Snowden, 1994; Simoncelli & Heeger, 1998; Derrington, 2000). Another view is that the visual system performs some type of feature matching, or tracking, over time (see for example, Movshon et al., 1985; Cavanaugh, 1992; Derrington, 2000). A third possibility is that the visual system determines motion direction from the spatial streaks created by temporal integration in the visual system when objects move with sufficient speed (Geisler, 1999). It is obvious that motion streaks are used to determine the motion path under some circumstances (e.g. when a sparkler moves quickly or when the electron beam in an oscilloscope moves quickly). These spatial representations of motion are created by temporal integration in the visual system. However, is this phenomenon general enough to be useful for determining the direction of object motion? Specifically, how fast must image features move before reliable motion streak signals are created in the visual system, and what types of features produce motion streak signals?

The motion streak hypothesis is illustrated schematically in Fig. 1. The figure shows the hypothetical responses of a population of neurons with receptive fields of different preferred orientations (at the same spatial location). The preferred orientation is indicated along the horizontal axis and the response is indicated on the vertical axis. Each symbol represents an individual cell (or group of cells) with a given preferred spatial orientation. The upper panel (Fig. 1A) shows the responses across the population for a feature

Address correspondence and reprint requests to: Wilson S. Geisler, Department of Psychology, Center for Vision and Image Sciences, University of Texas, Austin, TX 78712.

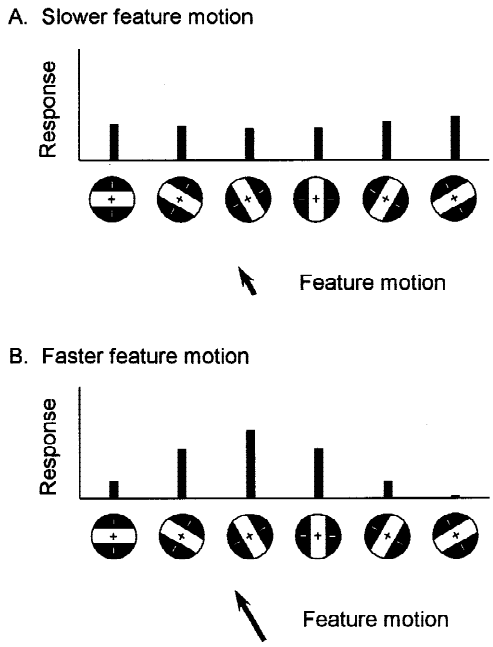

Fig. 1. Illustration of how the motion streak signals, produced by a moving feature (e.g. a small spot), might be encoded in a local population of orientation-selective neurons in primary visual cortex. The arrows indicate the vector of motion of the image feature; arrow length indicates the speed of motion and arrow orientation indicates the direction of motion. The horizontal axis plots the preferred spatial orientation of each local subpopulation of neurons. The vertical axis plots the pooled response of each subpopulation. These population responses include all of the direction-selective and nondirection-selective neurons. (A) The hypothesized distribution of response across preferred orientation for a feature moving at a speed less than the critical speed. Below the critical speed, the distribution of activity across all orientations is relatively flat. (B) The hypothesized distribution of response across preferred orientation for a feature moving at a speed greater than the critical speed. Above the critical speed, the distribution of activity peaks in the population of neurons whose receptive fields are oriented parallel to the direction of feature motion.

that is moving very slowly. The lower panel (Fig. 1B) shows the responses across the population for a feature that is moving faster. When the feature is moving slowly, similar responses are produced across all orientations. On the other hand, when the feature is moving quickly, there is a relative maximum at the orientation parallel to the direction of motion. This occurs because temporal integration creates a spatial streak (effectively, a bar) oriented parallel to the direction of motion. This relative maximum response in the distribution of activity across the population of cells encodes the direction of the moving feature, in much the same way that such a relative maximum encodes the orientation of a spatial contour.

Recently, Geisler (1999) reported psychophysical evidence that such motion streak signals are used by the human visual system to determine motion direction even at relatively low speeds (1 deg/s for small spots). In the main experiment, luminance detection thresholds were measured for a moving spot in the presence of dynamic random line masks oriented either parallel or perpendicular to the direction of spot motion. The target spot moved along a straight path for 250 ms, and a different random sample of line noise was presented in each frame. The logic of the experiment was as follows. If a moving spot produces a motion streak signal, then it should produce a larger response in the population of neurons whose orientation selectivity is parallel to the direction of motion, and hence, the parallel mask should be more effective in elevating threshold than the perpendicular mask. Geisler found that as spot speed increased, the threshold remained the same for both mask orientations until some critical spot speed was reached (approximately 12 spot-widths/s), beyond which the parallel mask became more effective. Geisler also reported computer simulations of cortical neuron responses to moving spots using the average spatio-temporal tuning functions that have been measured in the monkey with sine-wave grating stimuli (Geisler & Albrecht, 1997). These simulations suggest that the psychophysical results are consistent with what would be expected from the population response of neurons in the primary visual cortex.

The goal of the present study was to directly measure cortical neuron response properties that are relevant to the motion streak hypothesis. In the first experiment, we measured responses to a single moving spot that traveled either parallel or perpendicular to the spatial orientation of the receptive field (i.e. parallel or perpendicular to the elongated regions of the receptive field). If the responses of V1 neurons are consistent with the results of the psychophysical experiments, then the responses to a moving spot should become greater for motion parallel to the spatial orientation of the receptive field once a relatively low critical speed is exceeded. The results of the moving spot experiment agree with the prediction from the psychophysical experiments.

The key property of the visual system that is relevant to the motion streak hypothesis is the temporal integration parallel to the spatial orientation of the receptive field. Therefore, in the second experiment, we measured temporal tuning functions of cortical neurons using drifting plaid patterns (orthogonal contrast modulated sine-wave gratings). These plaid stimuli (which themselves are not expected to produce motion streaks) allowed us to quantitatively characterize the temporal and spatial tuning characteristics of cortical neurons for motion both parallel and perpendicular to the spatial orientation of the receptive field. The measurements for motion that is perpendicular to the spatial orientation of the receptive field are essentially equivalent to conventional measurements of spatial and temporal tuning with one-dimensional sine-wave gratings. However, little is known about the spatial and temporal characteristics of cortical neurons for motion parallel to the spatial orientation of the receptive field. Thus, these measurements provide new information that should be of general interest for understanding the spatial and temporal tuning properties of cortical cells, and are of specific interest to the motion streak hypothesis.

To help interpret the responses of cortical neurons to the spot and plaid stimuli, it is useful to consider the measured responses within the context of a common working model of cortical neurons. Over the past several decades, following the work of Hubel and Weisel (1962, 1968), a general consensus has developed on a model that can account for the response characteristics of cortical neurons; henceforth referred to as the "*standard model*." This model (which is defined in detail in the Methods section) combines linear filtering with three nonlinearities: contrast gain control, response expansion, and half-wave rectification (e.g. Movshon et al., 1978*a*; De Valois et al., 1982*a*; Hamilton et al., 1989; Albrecht & Geisler, 1991, 1994; Palmer et al., 1991; Emerson et al., 1992; Heeger, 1991, 1992*a*,*b*; DeAngelis et al., 1993, 1994; Gardner et al., 1999; for general reviews, see Robson, 1975; Shapley & Lennie, 1985; Carandini et al., 1999; Geisler & Albrecht, 2000). The work cited in the references above quantitatively

demonstrates that this model is consistent with many of the known properties of cortical neurons.

In general, we find that the expectations from the *standard model* are consistent with the measured responses to spots and the measured spatial and temporal tuning functions for motion that is parallel and perpendicular to the spatial orientation of the receptive field. There was, however, one noteworthy and unexpected exception: Many V1 neurons show direction selectivity for motion parallel to the spatial orientation of the receptive field. Although the results imply a somewhat more complicated mechanism for direction selectivity than is currently incorporated within the *standard model*, a relatively simple modification can produce this new type of direction selectivity.

Methods

Recording and physiology

The procedures for the paralyzed anesthetized preparation, the electrophysiological recording, the stimulus display, and the measurement of neural responses using systems analysis were similar to those described elsewhere (Hamilton et al., 1989; Albrecht & Geisler, 1991; Geisler & Albrecht, 1997; Metha et al., 2001). All experimental procedures were approved by the University of Texas at Austin Institutional Animal Care and Use Committee, and conform to the National Institutes of Health guidelines. In brief, young adult cats (*Felis domesticus*) and monkeys (*Macaca fascicularis* or *Macaca mulatta*) were prepared for recording under deep isoflurane anesthesia. Following the surgical procedures, isoflurane anesthesia was discontinued. Anesthesia and paralysis were maintained throughout the duration of the experiment using the following pharmaceuticals. For cats, anesthesia was maintained with sodium pentothal (2–6 mg/kg/h). For monkeys, anesthesia was maintained with sufentanil citrate (2–8 μg/kg/h). For both species, paralysis was maintained with gallamine triethiodide (10 mg/kg/h) and pancuronium bromide (0.1 mg/kg/h). The physiological state of the animal was monitored throughout the experiment by continuous measurement of the following quantitative indices: body temperature, inhaled/exhaled respiratory gases, pressure in the airway, fluid input, urine output, urinary pH, caloric input, blood glucose levels, electroencephalogram, and electrocardiogram. Microelectrodes were inserted into regions of the primary visual cortex such that the receptive fields of the neurons were located within 5 deg of the visual axis. Three different types of microelectrodes were utilized: varnish-insulated tungsten, glass pipette, or glass-coated platinum-iridium. The impedances of the microelectrodes ranged from 8 to 21 MΩ.

Stimulus presentation

In all the experiments reported here, the stimuli were confined to the conventional receptive field, which was determined by expanding the size of an optimal drifting sine-wave grating until the neuron's response stopped increasing (De Valois et al., 1985; DeAngelis et al., 1994). The stimuli were presented on a monochromatic Image Systems monitor at a frame rate of 100 Hz, with a mean luminance of 27.4 cd/m^2. To overcome the inherent nonlinearities in visual displays, both hardware and software methods were utilized to ensure a linear relationship between the requested luminance and the measured luminance. Standard orientation, spatial frequency, and spatial phase tuning functions were measured (using sine-wave grating patterns) to determine the optimal orientation, spatial frequency, and spatial phase. The stimulus was centered on the receptive field by finding the position of a half cycle of the optimal spatial frequency that produced the largest response. The stimuli were presented in a counterbalanced fashion such that all stimulus conditions occurred an equal number of times, in a random order. A single block consisted of 10 repeated presentations of the same stimulus condition. Each presentation was separated by a time interval equal to the duration of the presentation. Each block was separated by a time interval equal to the duration of the block. During these intervals, the animal viewed mean luminance. Generally, at least four blocks were obtained for each stimulus condition (resulting in 40 repeated temporal cycles); in some instances, as many as 20 blocks were obtained (resulting in 200 repeated temporal cycles).

Parallel motion and perpendicular motion

Once the preferred spatial orientation of a given receptive field was determined, measurements were made in four directions of motion for the spot stimuli (Fig. 2A) and for the plaid stimuli (Fig. 2B). The stimuli were moved either parallel to the preferred spatial orientation (referred to as "parallel motion"), or the stimuli were moved perpendicular to the preferred spatial orientation (referred to as "perpendicular motion"). For each of these two types of motion, parallel and perpendicular, the stimulus can be moved in each of two opposite directions (as indicated by the two-headed arrows). Thus, for example, if we assume that a hypothetical receptive field is oriented vertically (as illustrated in Fig. 2), then for parallel motion, the opposite directions are up and down, and for perpendicular motion, the opposite directions are left and right.

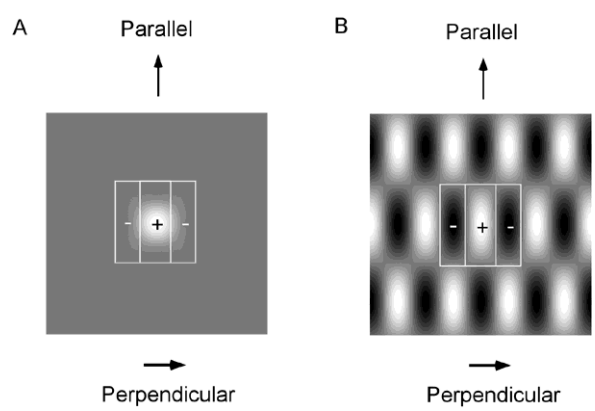

Fig. 2. Stimuli for measuring cortical cell responses for motion parallel to the spatial orientation of the receptive field, and for motion perpendicular to the spatial orientation of the receptive field. For parallel motion, the stimuli were moved in each of the opposite directions and similarly, for perpendicular motion the stimuli were moved in each of the opposite directions. This is indicated by the two-headed arrows. (A) Raised cosine spots. Measurements were made with light spots and dark spots. Spot width was set equal to the period of the optimal spatial frequency. (B) Orthogonal contrast modulated sine-wave gratings. These plaid patterns were created by multiplying a "carrier" component, oriented parallel to the spatial orientation of a given cell's receptive field, by a sine-wave "modulator" component, oriented perpendicular to the spatial orientation of a given cell's receptive field. Plaid patterns can also be described as the sum of two sine-wave components that differ in orientation. In this study, the plaid patterns were confined to the conventional receptive field (see Methods).

Moving spot experiment

Following the preliminary measurements (described above), we measured the responses to both a moving white spot (82 cd/m^2) and a moving black spot (4 cd/m^2). The velocity of the spot was parametrically varied, depending upon the width of the spot. The spot had a raised-cosine profile with a width equal to the period of the optimal spatial frequency. Although a spot of this width encroaches to some extent upon the inhibitory region(s) of the receptive field, the increased amount of light (or dark) in the excitatory region more than offsets the inhibition. For each stimulus condition, a spot of a given polarity (light or dark) was moved either parallel to or perpendicular to the preferred spatial orientation (see Fig. 2A). For parallel motion, the stimuli were moved in each of the opposite directions; similarly, for perpendicular motion, the stimuli were moved in each of the opposite directions.

Orthogonal contrast modulation experiment

In this experiment, we measured the response to orthogonal contrast modulated sine-wave gratings (plaids) moving either parallel or perpendicular to the preferred spatial orientation (see Fig. 2B). For parallel motion, the stimuli were moved in each of the opposite directions; similarly, for perpendicular motion, the stimuli were moved in each of the opposite directions. These plaid patterns can be described as the product of a pair of orthogonally oriented spatial sine-wave grating patterns (see Fig. 3):

$$L(x,y) = A\cos(2\pi f_y y)\cos(2\pi f_x x) + \bar{L}, \qquad (1)$$

where $\bar{L}$ is the mean luminance, A is the amplitude, f_x is the spatial frequency of the component aligned with the preferred spatial orientation of the cell, and f_y is the spatial frequency of the component orthogonal to the preferred spatial orientation of the cell. They can also be described as the sum of two sine-wave components of a particular frequency (f), differing by a particular orientation (2θ):

$$L(x,y) = \frac{A}{2}\cos(2\pi f\sin\theta y - 2\pi f\cos\theta x) + \frac{A}{2}\cos(2\pi f\sin\theta y + 2\pi f\cos\theta x) + \bar{L}, \qquad (2)$$

where $\theta = \tan^{-1}(f_y/f_x)$ and $f = \sqrt{f_x^2+f_y^2}$ (see Fig. 3). To simplify the presentation, we describe the plaid stimuli as contrast modulated gratings [e.g. eqn. (1)].

Using these patterns, we were able to measure a cell's temporal-frequency tuning and spatial-frequency tuning for parallel motion as well as perpendicular motion. The temporal and spatial tuning functions for perpendicular motion were measured by varying the temporal and spatial frequency of the sine-wave component whose orientation was aligned parallel with the cell's preferred spatial orientation. (In other words, the motion was perpendicular to the elongated regions of the receptive field, and the orientation of the parametrically varied spatio-temporal component was parallel to the elongated regions of the receptive field.) The temporal and spatial tuning functions for parallel motion were measured by varying the temporal and spatial frequency of the sine-wave component whose orientation was aligned perpendicular to the cell's preferred spatial orientation. (In other words, the motion was parallel to the elongated regions of the receptive field, and the orientation of the parametrically varied spatio-temporal component was perpendicular to the elongated regions of the receptive field.) Note that these stimuli are equivalent to rigid moving plaid patterns (which is how they appear subjectively to a human observer).

When measuring the temporal tuning functions, the spatial frequency of the sine-wave component aligned with the cell's preferred spatial orientation was set to the cell's optimal value, u_c, determined from preliminary measurements, and the orthogonal component was set to $u_c/3$ [i.e. $f_x = u_c$ and $f_y = u_c/3$ in eqn. (1)]. When measuring the spatial tuning functions for perpendicular motion, the spatial frequency of the sine-wave component orthogonal to the cell's preferred spatial orientation was fixed at $u_c/3.5$, and the temporal frequency was set to the optimal value, w_c. When measuring the spatial tuning functions for parallel motion, the spatial frequency of the sine-wave component aligned with the cell's preferred spatial orientation was fixed at u_c, and the temporal frequency was set to w_c.

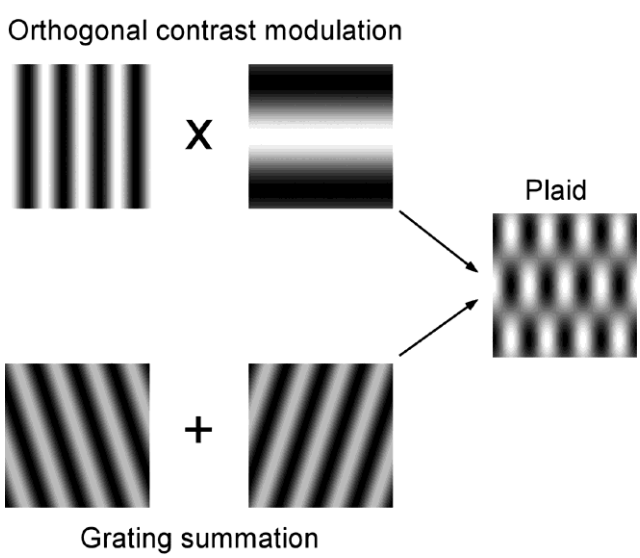

Fig. 3. Illustration of two equivalent methods for constructing plaid patterns. The plaid patterns used in this study can be constructed by multiplying two orthogonally oriented sine-wave gratings with different spatial frequencies (one optimized for the length of the receptive field and one optimized for the width). Equivalently, the plaid patterns can be constructed by summing two sine-wave gratings of the same spatial frequency, with some particular difference in orientation.

Quantitative predictions

To help interpret the experimental results, we simulated the responses of primary visual cortex neurons using the *standard model*. This model consists of a linear spatio-temporal mechanism (Movshon et al., 1978*a*; Watson & Ahumada, 1985), plus three nonlinear mechanisms: contrast normalization, half-wave rectification, and a response exponent (Albrecht & Geisler, 1991; Heeger, 1991). It has been demonstrated that this model adequately describes many aspects of single neuron responses in the primary visual cortex (e.g. Movshon et al., 1978*a*; De Valois et al., 1982*a*; Hamilton et al., 1989; Albrecht & Geisler, 1991, 1994; Palmer et al., 1991; Emerson et al., 1992; Heeger, 1991, 1992*a*,*b*; DeAngelis et al., 1993, 1994; Gardner et al., 1999; for general reviews, see Robson, 1975; Shapley & Lennie, 1985; Carandini et al., 1999; Geisler & Albrecht, 2000). However, as will be

demonstrated in the Results section, we found that, in addition to the well-established property of "perpendicular motion direction selectivity," many cortical neurons also show the previously unreported property of "parallel motion direction selectivity." Therefore, it was necessary to generalize the *standard model* such that it could also account for parallel motion direction selectivity.

The *single axis* linear spatio-temporal filter proposed by Watson and Ahumada (1985) is described by a transfer function of the following form:

$$H(u,v,w) = H_x(u)H_y(v)H_t(w)[q_x - (1 - q_x)sign(u)sign(w)], \tag{3}$$

where $H_x(u)$ is a spatial filter in the x direction, $H_y(v)$ is a spatial filter in the y direction, and $H_t(w)$ is a temporal filter. The parameter q_x determines the direction selectivity for motion along the x axis. (Note that the *sign* function has a value of $+1$ for arguments greater than zero, and a value of -1 for arguments less than zero.) In modeling cortical neurons, the y axis corresponds to the long axis of the spatial receptive field, and hence, the direction selectivity is for perpendicular motion.

The *double axis* linear spatio-temporal filter proposed here contains another parameter, q_y, which determines the direction selectivity for motion along the y axis:

$$H(u,v,w) = H_x(u)H_y(v)H_t(w)[q_x - (1 - q_x)sign(u)sign(w)] \times [q_y - (1 - q_y)sign(v)sign(w)]. \tag{4}$$

This *double axis* direction-selective filter reduces to the *single axis* direction-selective filter by setting $q_y = 1.0$, and reduces to a nondirection-selective filter by setting $q_x = 1.0$ and $q_y = 1.0$. For example, setting $q_x = 0.5$ and $q_y = 1.0$ yields a receptive field that is highly direction selective along the x axis and nondirection selective along the y axis; setting $q_x = 1.0$ and $q_y = 0.5$ yields a receptive field that is highly direction selective along the y-axis and nondirection selective along the x axis; setting $q_x = 0.5$ and $q_y = 0.5$ yields a receptive field that is highly direction selective along both the x axis and the y axis.

To simulate simple cell responses, $H_x(u)$ was taken to be the transform of a log Gabor function, $H_y(v)$ the transform of a Gaussian function, and $H_t(w)$ the transform of a difference of gamma functions (Watson & Ahumada, 1985). The output of the linear filter was then half-wave rectified and taken to an exponent of 2.0. To simulate complex cell responses, we obtained the outputs of two linear filters: one with the log Gabor function in cosine phase and one with the log Gabor function in sine phase. The outputs of these two filters were each squared and then summed (Adelson & Bergen, 1985; van Santen & Sperling, 1985). Because the contrast was held constant in our experiments, the contrast normalization (pooled divisive inhibition) was constant, and played no role in the predictions. Also, for the particular results reported here, the predictions for the simulated simple and complex cell responses are identical, and hence, are not reported separately.

Results

Moving spot experiment

Fig. 4 shows the responses of a representative neuron (recorded from the primary visual cortex of a monkey) for the moving spot experiment. The speed of the spot motion (in spot-widths/s) is plotted on the horizontal axis, and the ratio of the responses for parallel *versus* perpendicular motion is plotted on the vertical axis.

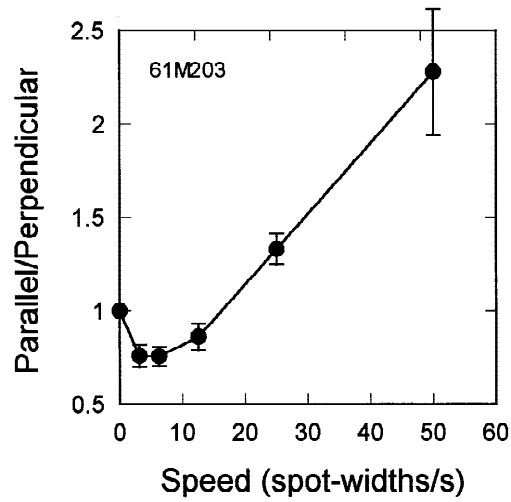

Fig. 4. Response of a representative neuron in the monkey visual cortex to a moving spot. The vertical axis plots the response amplitude for parallel motion divided by the response amplitude for perpendicular motion. The horizontal axis plots the spot speed in spot-widths/s. The spot width was set to the preferred spatial period of the receptive field (i.e. one over the preferred spatial frequency).

The response ratio was obtained in the following fashion. First, the responses for the opposite directions of parallel motion were summed; then, the responses for the opposite directions of perpendicular motion were summed; finally, the ratio of the sums was computed. When the ratio is greater than 1.0, then the response is greater for the spot moving parallel to the spatial orientation of the receptive field. As can be seen, the response ratio increases as the spot speed increases, and clearly exceeds 1.0 at the higher speeds. This pattern of results was found in all of the cells, for both cat and monkey. To summarize the results for the entire sample, the ratio of the responses to parallel *versus* perpendicular motion was averaged across all 45 experiments; this average ratio is plotted in Fig. 5A.

The dashed curve in Fig. 5A shows the simulated responses of an average cortical neuron in primary visual cortex. These predictions were obtained using the *standard model* (see Methods). These are parameter-free predictions that were generated directly from the average tuning characteristics of monkey primary visual cortex neurons (reported in Geisler & Albrecht, 1997). The specific average values used in the simulations were an orientation bandwidth of 40 deg, a spatial frequency bandwidth of 1.5 octaves, a preferred temporal frequency of 8 Hz, a temporal frequency bandwidth of 2.5 octaves, a nonlinear response exponent of 2.0, a base rate of 0.8 spikes/s, and a direction selectivity of 0.6 (for perpendicular motion). These average tuning parameters are very similar to the averages reported by others (e.g. De Valois et al., 1982*a*,*b*; Foster et al., 1985; Hamilton et al., 1989; Hawken et al., 1996). The predicted response ratios display the major trends in the data.* The lack of a perfect fit between the predictions from the

*In the description of the results of the orthogonal contrast modulation experiment, we report that the average direction selectivity for parallel motion is approximately half the average direction selectivity for perpendicular motion. We found a similar relationship in the responses to moving spots. Therefore, we also generated predictions for a *double axis* direction-selective filter (see Methods) with direction selectivities of 0.6 and 0.3. These predictions are not shown because they are essentially identical to the dashed curve in Fig. 5A.

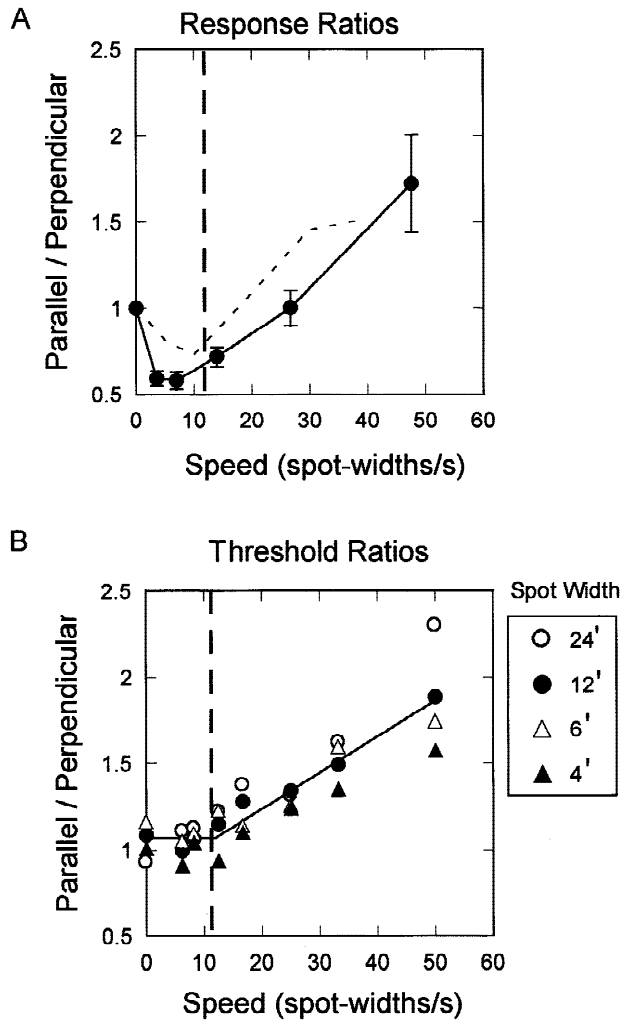

Fig. 5. Physiological and behavioral responses to moving spots. A total of 45 experiments was performed on 14 neurons recorded from within V1 (9 cat neurons and 5 monkey neurons). (A) Neurophysiological responses of the entire sample of neurons to moving spots. The vertical axis plots the average response amplitude for parallel motion divided by the average response amplitude for perpendicular motion. The horizontal axis plots the spot speed in spot-widths/s. For each cell, the spot width was set to the preferred spatial period of the receptive field (i.e. one over the preferred spatial frequency). The dashed curve shows parameter-free predictions based upon the average tuning characteristics of cortical cells reported in Geisler and Albrecht (1997). For these predictions, it was assumed that the cell was only direction selective for perpendicular motion. (B) Human psychophysical detection thresholds for moving spots superimposed on dynamic random line masks oriented either parallel to or perpendicular to the direction of spot motion (data taken from Geisler, 1999). The vertical axis plots the ratio of the threshold for the parallel mask to the threshold for the perpendicular mask. The horizontal axis plots spot speed in spot-widths/s. The data points represent the average thresholds from two subjects. The vertical lines in both panels indicate the average speed beyond which the threshold ratio increases (the "critical speed" reported in Geisler, 1999).

large sample of monkey cells and the measured responses from this specific sample of cells is not particularly surprising given the substantial heterogeneity in the tuning characteristics of neurons in the primary visual cortex.

For comparison, Fig. 5B summarizes the results for the two subjects in the previously published psychophysical study. The spot speed (in spot-widths/s) is plotted on the horizontal axis, and the ratio of thresholds (for the motion that is parallel *vs.* perpendicular to the orientation of the mask) is plotted on the vertical axis. The different symbols are for spots of different widths; each symbol represents the average threshold ratio for the two subjects. The vertical dashed line (plotted in Figs. 5A and 5B) shows the average critical speed (12 spot-widths/s) across all spot sizes, for both subjects. Below the critical speed, the threshold ratio is approximately constant; above the critical speed, the threshold ratio increases approximately linearly. In the neurophysiological experiment, the critical speed and the rate at which the response ratio increases with spot speed are quite similar to the critical speed and the rate at which the threshold ratio increases in the psychophysical experiment. The primary difference between the neurophysiological and psychophysical results is that the neurophysiological response ratio drops below 1.0 at low spot speeds.

In sum, the measured responses of single neurons to moving spots suggest that motion streak signals exist in the primary visual cortex. Further, the cortical responses, in both cat and monkey, appear to be consistent with the human psychophysical results and with the parameter-free predictions from the *standard model*. However, because the motion streak hypothesis is fundamentally dependent upon the temporal-frequency tuning for parallel motion, and because the standard model is based upon measurements of the tuning for perpendicular motion, it seemed prudent to also measure the tuning for parallel motion. To do this we used plaid patterns, which closely match the spatial properties of the receptive fields and hence produce robust responses.

Orthogonal contrast modulation experiment

Figs. 6A and 6B show the spatial-frequency tuning functions of a representative neuron (recorded from the primary visual cortex of a monkey) for parallel and perpendicular motion of plaid patterns. The responses for perpendicular motion are shown in Fig. 6A, averaged across the opposite directions of motion (as indicated by the double-headed arrow). The responses for parallel motion are shown in Fig. 6B, averaged across the opposite directions of motion. Recall that for perpendicular motion, we varied the spatial frequency of the component whose orientation was aligned parallel with the cell's preferred orientation; whereas for parallel motion, we varied the spatial frequency of the component whose orientation was aligned perpendicular to the preferred orientation.

The temporal-frequency tuning functions for the same neuron are shown in Figs. 6C–6F. The responses for one direction of perpendicular motion are shown in Fig. 6C and the responses for the opposite direction of perpendicular motion are shown in Fig. 6D. The responses for one direction of parallel motion are shown in Fig. 6E and the responses for the opposite direction of parallel motion are shown in Fig. 6F.

There are four important properties that can be seen in the responses of the representative neuron shown in Fig. 6. The first three properties are general: They hold true for the entire sample of neurons. The fourth property, however, is not general.

1. The shape of the spatial tuning function for perpendicular motion is quite different from the shape of the spatial tuning function for parallel motion: For perpendicular motion, the tuning is band pass (Fig. 6A), whereas for parallel motion, the tuning is low pass (Fig. 6B).

2. The shape of the temporal tuning function is quite similar for both parallel motion and perpendicular motion: The solid

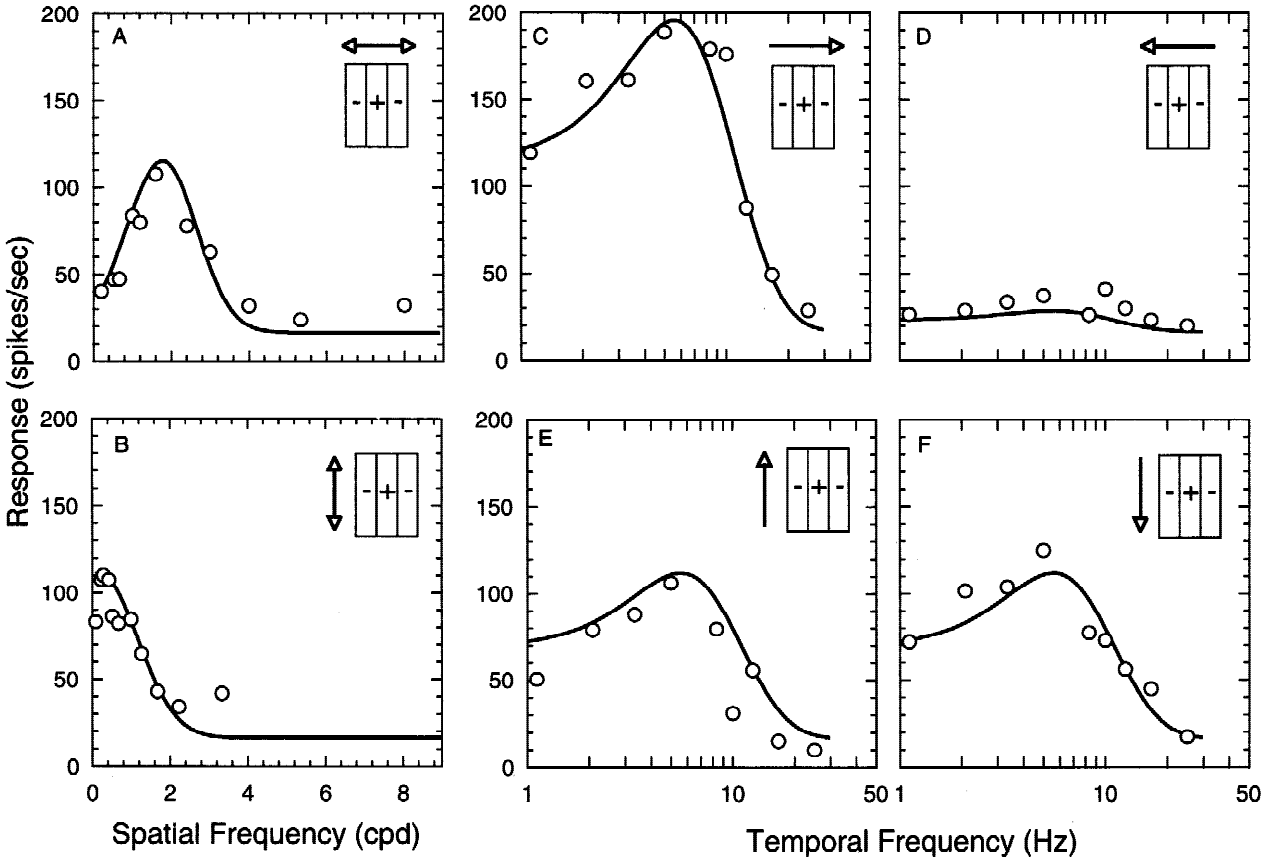

Fig. 6. Responses of a representative neuron in the monkey visual cortex to orthogonal contrast modulated gratings (plaids). (A) Responses for perpendicular motion as a function of spatial frequency. The responses for the opposite directions were averaged. (B) Responses for parallel motion as a function of spatial frequency. The responses for the opposite directions were averaged. (C & D) Responses for perpendicular motion as a function of temporal frequency. The responses for the opposite directions are plotted separately. (E & F) Responses for parallel motion as a function of temporal frequency. The responses for the opposite directions are plotted separately. The solid curve in each panel shows the predictions from the *standard model* of striate cortex neurons (see text for details).

curves (in Figs. 6C–6F) are identical in shape and only differ by a vertical scale factor.

3. The amplitude of the temporal tuning function for perpendicular motion, averaged across the opposite directions, is approximately equal to the amplitude of the temporal tuning function for parallel motion, averaged across the opposite directions: The average of the solid curves in Figs. 6C and 6D is identical to the average of the solid curves in Figs. 6E and 6F.

4. This particular neuron is direction selective for perpendicular motion, but it is not direction selective for parallel motion.

Now, consider the entire sample of cells.

First, consider the shapes of the spatial tuning functions for parallel and perpendicular motion. To quantify the differences in the shapes of the spatial tuning functions for the entire sample of cells, we computed (for each cell) the rank-order correlation coefficient for response amplitude and spatial frequency. (Given a perfectly low pass function, the coefficient will be -1.0; whereas, given a perfectly band pass function, the coefficient will be 0.0.) For this sample of neurons, the average rank-order correlation coefficient for perpendicular motion was -0.7, and for parallel motion it was -0.15. The results of this analysis indicate that the spatial tuning is approximately band pass for perpendicular motion and low pass for parallel motion.

Second, consider the shapes of the temporal tuning functions for parallel and perpendicular motion. To quantify the similarity in the shapes of the temporal tuning functions, we computed (for each cell) the correlation coefficient of the response amplitude for parallel motion and the response amplitude for perpendicular motion. Fig. 7A shows a scatter plot of the response amplitude of the cell shown in Fig. 6, for parallel *versus* perpendicular motion. If the temporal tuning functions are identical in shape, then the responses should fall on a straight line through the origin with a slope equal to the average ratio of the responses. The degree to which the two sets of points fall along a straight line can be quantified by the Pearson correlation coefficient (r). As indicated in the figure, the correlation coefficient for this cell is quite high ($r = 0.88$), and thus, on average, the points fall close to the straight line. A histogram of the correlation coefficients for this sample of neurons is shown in Fig. 7B. As can be seen, for most of the cells, the correlation coefficients are quite high. The results of this analysis indicate that the shapes of the temporal tuning functions are quite similar for parallel motion and perpendicular motion.

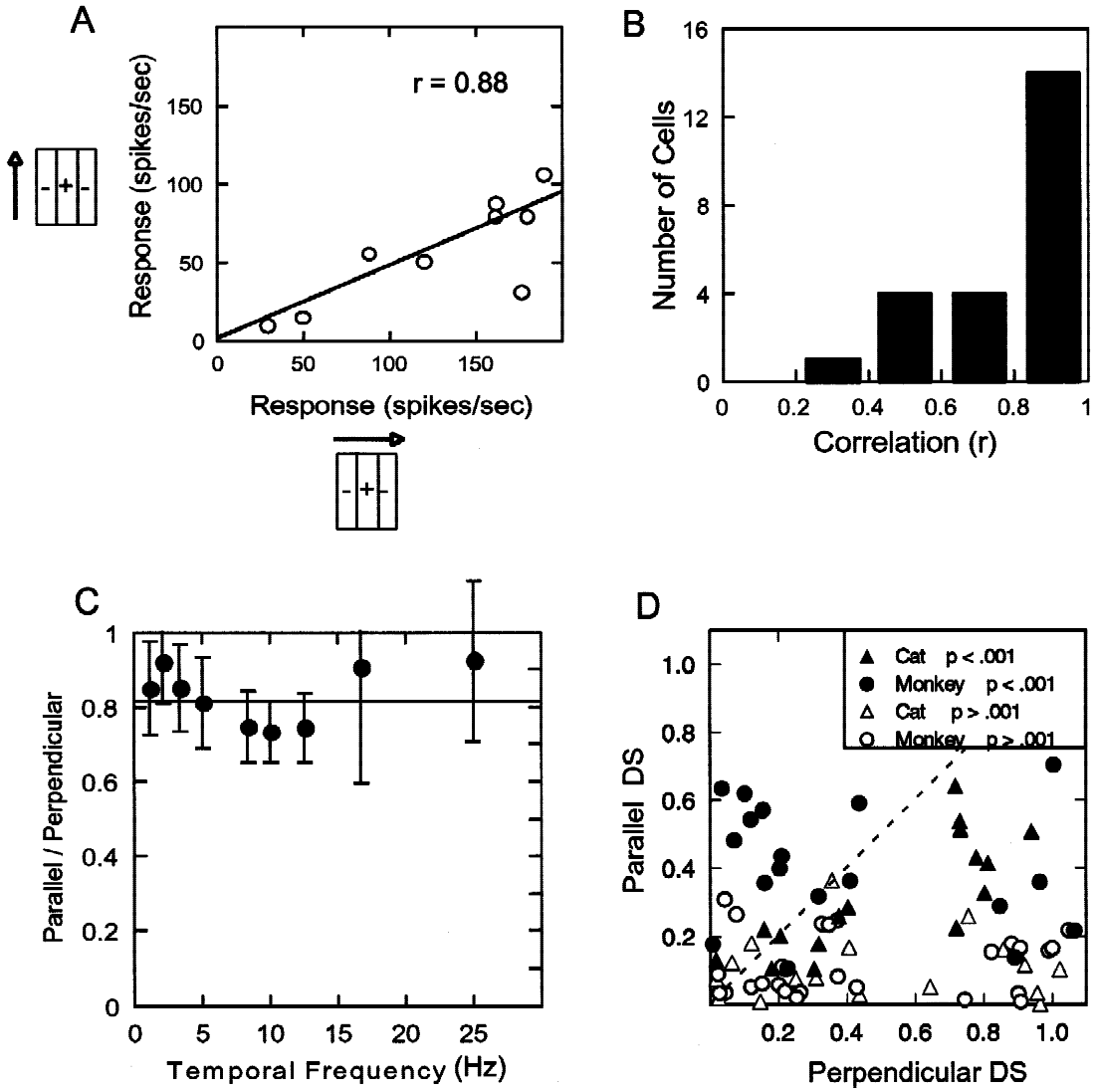

Fig. 7. Summary of responses of cat and monkey neurons to orthogonal contrast modulated gratings (plaids). Seventy-seven experiments were performed on 28 neurons (21 complex cells and 7 simple cells) recorded from within V1 (17 cat neurons and 11 monkey neurons). (A) The response amplitude of a representative neuron for parallel motion is plotted as a function of the response amplitude for perpendicular motion; these were taken from the temporal-frequency tuning measurement in the preferred direction. If the shapes of the temporal-frequency tuning functions are the same for both parallel and perpendicular motion, then the points should fall on a straight line through the origin. The degree to which this holds is given by the Pearson correlation coefficient (r). As indicated in the panel, for this cell, $r = 0.88$. (B) Histogram showing the correlation coefficients for the entire sample. (C) The ratio of the responses for parallel *versus* perpendicular motion at each temporal frequency, averaged across the entire sample of cells. The error bars indicate ± 2 standard errors. Note that unlike the responses to moving spots, the response ratio remains constant independent of speed (cf. Fig. 3A). (D) The direction selectivity index for parallel motion is plotted as a function of the direction selectivity index for perpendicular motion. The solid symbols represent experiments where the direction selectivity for parallel motion was statistically significant (at the 0.001 level of confidence), in comparison to what would be expected from chance alone. (Statistical significance for perpendicular motion is not shown.) For those points above the dashed diagonal line, the direction selectivity was greater for parallel motion than it was for perpendicular motion.

Third, consider the similarity of the average response amplitudes of the temporal-frequency tuning functions for parallel and perpendicular motion. To quantify this property, we computed (for each cell) two average temporal tuning functions: one for parallel motion (averaged across the opposite directions) and one for perpendicular motion (averaged across the opposite directions). We then took the ratio of the two average temporal tuning functions at each temporal frequency. If the average response amplitude for parallel motion is equal to the average response amplitude for perpendicular motion, then the ratio of the averages should be constant and equal to 1.0, at all temporal frequencies. For the cell shown in Fig. 6, this ratio is equal to 0.81. The results for the sample as a whole are summarized in Fig. 7C, which plots the ratio (± 2 standard errors) for each temporal frequency, averaged across all cells. As can be seen, the ratio is approximately constant across temporal frequency; as indicated by the horizontal line, the mean

was 0.82. The results of this analysis indicate that the average response amplitude for parallel and perpendicular motion is nearly the same across a wide range of temporal frequencies.

Fourth, consider the property of direction selectivity for parallel and perpendicular motion. Fig. 7D shows a scatter plot of the direction selectivity index:† Direction selectivity for perpendicular motion is plotted along the horizontal axis, and direction selectivity for parallel motion is plotted along the vertical axis. Many neurons show direction selectivity for perpendicular motion and essentially no direction selectivity for parallel motion (similar to the cell illustrated in Fig. 6). Surprisingly, however, many of the cells show direction selectivity for parallel motion. The solid symbols in the plot show the cases where the direction selectivity index for parallel motion was significantly greater than zero ($P < 0.001$).‡ Particularly surprising is the fact that some cells are considerably more direction selective for parallel motion than they are for perpendicular motion (see data points above the dashed line). The results of this analysis demonstrate that some neurons are more direction selective for perpendicular motion, other neurons are more direction selective for parallel motion, and many neurons are direction selective for both parallel and perpendicular motion. It is worth noting that this same pattern of direction selectivity was observed for the moving spot measurements: The range of direction selectivity for parallel motion is approximately 2/3 of that for perpendicular motion.

Now, consider the expectations from the *standard model* (the conventional *single axis* direction-selective filter described in detail in the Methods) for the spatial- and temporal-frequency tuning functions measured with plaid patterns. The solid curves through the data points for the neuron illustrated in Fig. 6 are the predictions from the *standard model*. For these predictions, several parameters were allowed to vary: the optimal spatial and temporal frequency, the spatial- and temporal-frequency bandwidth, the base rate, and the direction selectivity. As can be seen, the predictions from the *standard model* are quite good for this representative neuron, particularly given the fact that the exact same set of parameters was used to generate the curves in all six panels.

In general, independent of the particular parameter values, the *standard model* predicts the following:

1. The spatial-frequency tuning function is band pass for parallel motion and low pass for perpendicular motion.
2. The shape of the temporal-frequency tuning function is the same for both parallel and perpendicular motion.
3. The temporal tuning functions, when averaged across the opposite directions, are identical for both parallel and perpendicular motion.
4. The responses for the opposite directions of parallel motion are equal (i.e. the direction selectivity index for parallel motion is zero).

All but the last prediction hold approximately for the population as a whole.

Parallel motion direction selectivity

The most significant departure from the predictions of the *standard model* is that many cells show some degree of direction selectivity for parallel motion (see Fig. 7D). There are several possible explanations for this unexpected result.

One possible explanation for the parallel motion direction selectivity that we have observed is the stochastic nature of cortical neurons. Specifically, given any variability in the response, and a finite sample of measurements, the direction selectivity index will almost always be greater than zero, even for a cell that has no direction selectivity. To assess whether the response variability of the neurons could account for the high degrees of parallel motion direction selectivity observed in this sample, we performed the analysis described in footnote‡. This statistical analysis of the responses revealed that the parallel motion direction selectivity for many cells was greater than what would be expected by chance alone (with a confidence level of 99.9%). Thus, it seems unlikely that response variability can account for the parallel motion direction selectivity that we have measured.

A second possible explanation is imprecise alignment of the plaid pattern with respect to the preferred spatial orientation of a neuron's receptive field. Such misalignment will introduce errors into the measurements of parallel motion direction selectivity for any neuron that shows a high degree of perpendicular motion direction selectivity. Specifically, the misalignment will introduce spurious parallel motion direction selectivity. In the present set of experiments, the optimal orientation was quantitatively determined from a preliminary measurement of the cell's orientation tuning function, in order to ensure correct orientation alignment of the plaid patterns. This procedure provided a precise estimate of the preferred orientation: The average 95% confidence interval for the preferred orientation was ±2.3 deg, and no cell had a 95% confidence interval that exceeded ±5 deg. Nonetheless, to assess the potential effect of orientation misalignment, we used the *single axis standard model* to estimate the expected responses of a neuron (with varying degrees of perpendicular motion direction selectivity) to parallel motion, as a function of the degree of orientation misalignment. The results of this analysis show that a misalignment of ±5 deg introduces only a minor amount of spurious parallel motion direction selectivity in the measurements, even for a neuron with a high degree of perpendicular motion direction selectivity. Furthermore, even large orientation misalignments could not account for the neurons that were equally or more direction selective for parallel motion than for perpendicular motion (see Fig. 7D).

We are therefore left with a third possible explanation: Simply, many cortical neurons are direction selective for motion parallel to their receptive field. Fig. 8 shows the temporal-frequency tuning

†The direction selectivity index is defined as $1 - (r_{np} - r_0)/(r_p - r_0)$, where r_{np} is the response in the nonpreferred direction, r_p is the response in the preferred direction, and r_0 is the base rate (which was generally quite small).

‡These statistical tests were performed as follows. First, the temporal tuning function for parallel motion was obtained by averaging the responses for the opposite directions of motion. Next, the variance proportionality constant was determined from the ratio of the variance to the mean across all the measured responses. Using the average temporal tuning function, and the variance proportionality constant, two random examples of the tuning function were generated using the same number of stimulus repetitions that occurred in the actual experiment (typically 40 repetitions). From these two randomly generated tuning functions we computed the value of the direction selectivity index. The above computations were repeated 20,000 times to obtain the sampling distribution for the direction selectivity index, under the null hypothesis that there was no direction selectivity. The sampling distribution was evaluated to determine the magnitude of direction selectivity that would be required for a significance level of 0.001; that is, this direction selectivity index would have been exceeded by chance with a probability of less than 0.001, a 99.9% level of confidence. Several other forms of statistical test were also tried and the results were nearly identical.

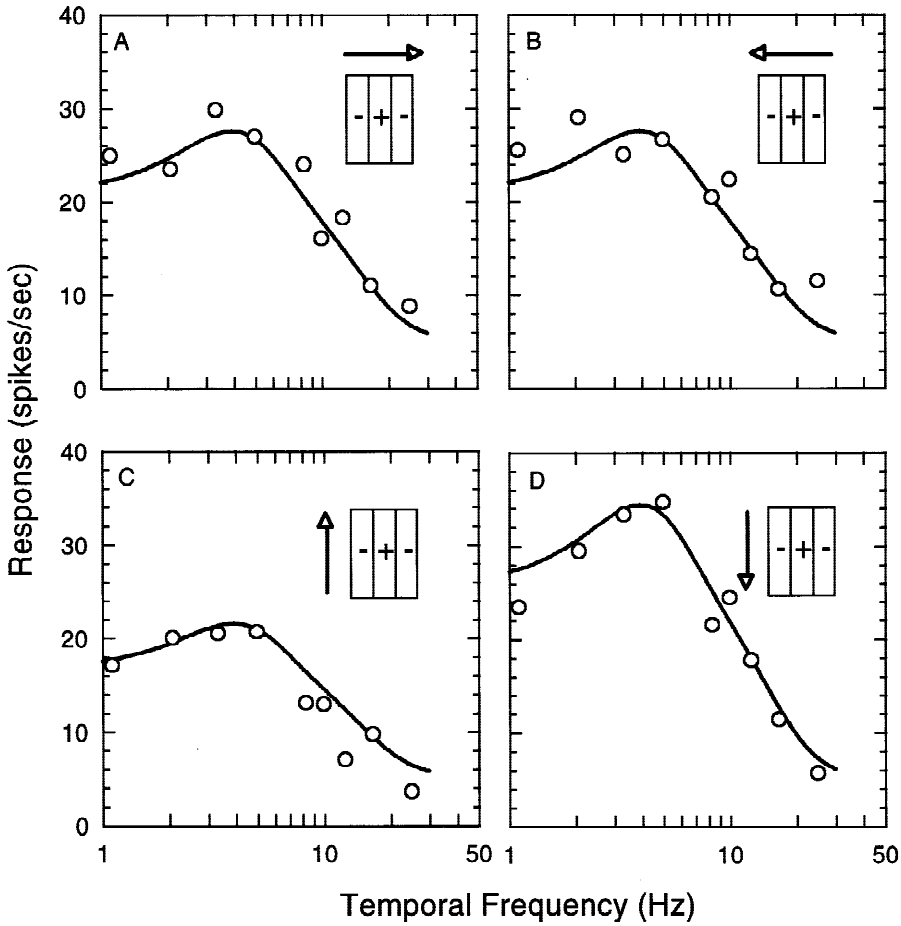

Fig. 8. Responses (to plaid patterns) of a representative neuron in the monkey visual cortex that had direction selectivity for parallel motion. (A & B) Responses for perpendicular motion as a function of temporal frequency, in each of the opposite directions. (C & D) Responses for parallel motion as a function of temporal frequency, in each of the opposite directions. This neuron is not direction selective for perpendicular motion; it is, however, direction selective for parallel motion. The solid curve in each panel shows the predictions of a linear spatio-temporal filter with a *single-axis* direction-selective mechanism tuned for motion that is parallel to the spatial orientation of the receptive field (see text for details).

functions of a monkey V1 neuron for both parallel motion and perpendicular motion of a plaid pattern. As can be seen, the responses are nearly identical for the opposite directions of perpendicular motion (Figs. 8A and 8B), but the responses are quite different for the opposite directions of parallel motion (Figs. 8C and 8D). Fig. 9 shows the temporal-frequency tuning functions of a neuron with approximately equal levels of direction selectivity for both parallel motion and perpendicular motion. Taken together, the results illustrated in Figs. 7D, 8, and 9 indicate that many cortical neurons may well be direction selective for parallel motion.

Discussion

Summary of the present work

Recent human psychophysical evidence supports the hypothesis that one of the cues the visual system has available to determine motion direction is the spatial orientation responses produced by motion streaks (Geisler, 1999). Further, computer simulations based upon the *standard model* of V1 neurons (Geisler, 1999) have suggested that these spatial orientation responses may be encoded by the orientation-selective neurons in primary visual cortex. Specifically, the simulations showed that if a natural feature moves at a sufficient velocity, it should produce the largest responses in those V1 neurons whose preferred spatial orientation is parallel to the direction of motion. This relative maximum response in the distribution of activity across preferred spatial orientation would encode the direction of the moving feature (see Fig. 1).

The aim of the present study was to obtain neurophysiological data relevant to the motion streak hypothesis. To this end, we measured the responses of cortical neurons for motion that was perpendicular to, and motion that was parallel to, the preferred spatial orientation of each neuron's receptive field (see Fig. 2). The responses to moving spots were measured as a function of velocity, and the responses to plaid patterns were measured as a function of the temporal frequency and the spatial frequency of the two sine-wave components.

The results of the moving spot experiment are consistent with the hypothesis that motion streak signals exist in the primary visual cortex. Specifically, as the speed of spot motion increases, the response of a V1 neuron to parallel motion increases while the response to perpendicular motion decreases; ultimately, the response becomes greater for parallel motion than for perpendicular motion (see Figs. 4 and 5A). Thus, when the motion of a feature in a natural visual scene exceeds some critical value, it will produce larger responses in those V1 neurons oriented parallel to the direction of motion than in those oriented perpendicular to the direction of motion. These results are consistent with the psychophysical evidence for motion streak signals in the human visual system (see Fig. 5B). Further, the results are also consistent with the computer simulations, based upon the *standard model*, which predict that motion streak signals should exist in V1 neurons.

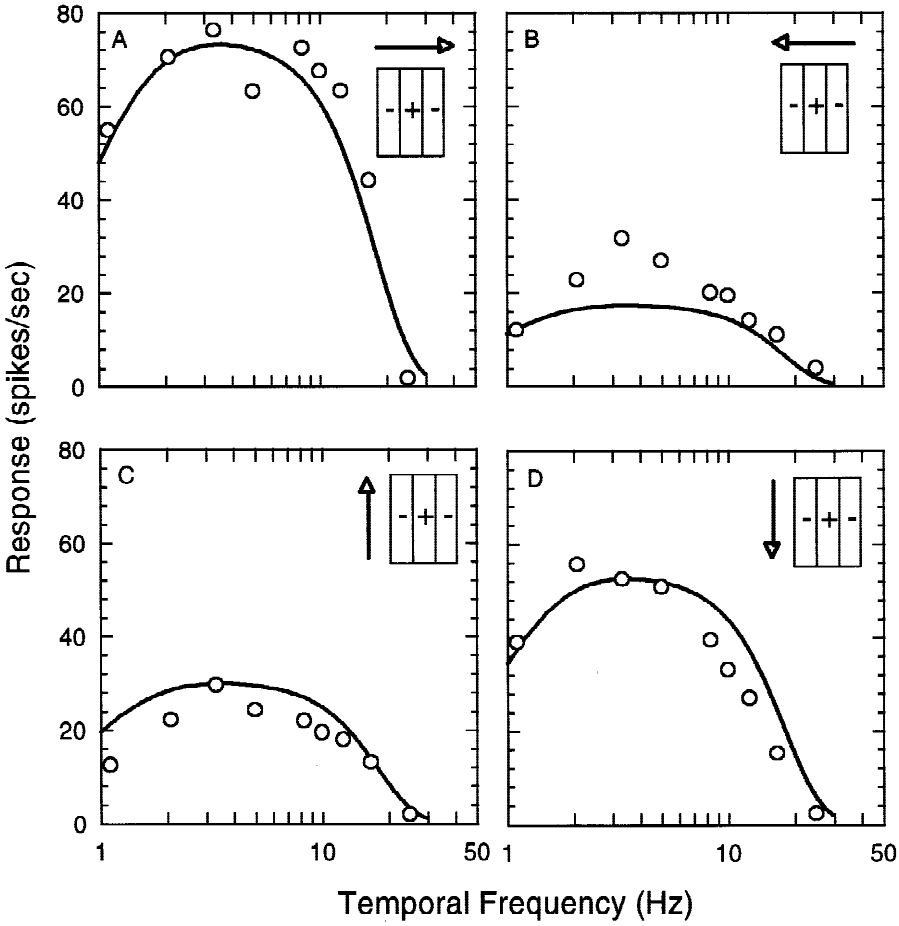

Fig. 9. Responses (to plaid patterns) of a representative neuron in the monkey visual cortex that had direction selectivity for both parallel motion and perpendicular motion. (A & B) Responses for perpendicular motion as a function of temporal frequency, in each of the opposite directions. (C & D) Responses for parallel motion as a function of temporal frequency, in each of the opposite directions. This neuron is direction selective for perpendicular motion and it is also direction selective for parallel motion. The solid curve in each panel shows the predictions of a linear spatio-temporal filter with a *double-axis* direction-selective mechanism, which is simultaneously tuned for both perpendicular and parallel motion (see text for details).

However, the strength of the argument for the motion streak hypothesis, based solely upon the measured responses to moving spots, is weakened by the fact that the *standard model* was primarily developed based upon the measurements of responses to motion that was perpendicular to the spatial orientation of the receptive field (that is, to one-dimensional gratings that were moving perpendicular to the orientation of the receptive field or to one-dimensional gratings that were counterphase flickering[§]), and hence, the predictions of the *standard model* may not be appropriate for parallel motion.

To address this concern, we measured the responses of V1 neurons to plaid patterns because plaid patterns produce robust responses from cortical neurons, and plaid patterns make it possible to measure the spatial and temporal tuning characteristics of cortical neurons for motion that is parallel to the orientation of the receptive field. The results of the present study show that the measured responses of V1 neurons to plaid patterns are robust (see Figs. 6–9). Further, the responses to plaid patterns are in good agreement with the responses to moving spots. Finally, with the exception of the rather surprising finding that some neurons show direction selectivity for parallel motion, the responses are in good agreement with the expectations from the *standard model*.

[§]Recall that a counterphase flickering grating is equivalent to the sum of two gratings drifting in opposite directions.

There is one apparent contradiction between the measured responses to spots moving at different speeds and the measured responses to plaids moving at different speeds. In particular, as the speed of a moving spot increases, the ratio of the responses to parallel *versus* perpendicular motion increases (see Figs. 4 and 5A). In contrast, as the speed of a moving plaid increases, the ratio of the responses to parallel *versus* perpendicular motion remains approximately constant (see Fig. 7C). Despite this apparent contradiction, this difference in the responses to spots and plaids is actually consistent with the expectations from the *standard model*. This is because, unlike the motion streak signals that are produced by moving spots (and most other moving patterns in natural scenes), moving plaid patterns should not produce motion streak signals.** Thus, the *standard model* predicts that the ratio of the responses to parallel *versus* perpendicular motion should be constant as a function of speed for moving plaids, even though it increases as a function of speed for moving spot stimuli.

In sum, based upon the measured responses to spots and plaids moving parallel and perpendicular to the preferred spatial orientation of the receptive fields, we can conclude that the oriented spatial motion signals available in natural images produce oriented

**As the speed of a plaid pattern increases, and the white–black spatial variations in the plaid pattern are integrated through time (due to the temporal integration of the visual system), the net effect is to simply reduce the contrast to zero.

spatial motion streak signals in the population response of striate cortex neurons.

Parallel and perpendicular direction selectivity

In contrast to our expectations, based upon the neurophysiological literature and the predictions from the *standard model*, we found that many cortical neurons appear to display some degree of direction selectivity for motion parallel to the receptive field (see Figs. 6–9). Even more surprising is the finding that for some neurons the direction selectivity for parallel motion was observed to be greater than the direction selectivity for perpendicular motion. The conventional *single axis* direction-selective filter incorporated within the *standard model* cannot account for these results.

It is possible that the mechanism for parallel direction selectivity is similar to the mechanism for perpendicular direction selectivity. It has long been thought that perpendicular direction selectivity is the result of certain combinations of nondirection-selective inputs that are position (or phase) shifted appropriately in space and time (Reichardt, 1961; Barlow & Levick, 1965). The conventional view of direction selectivity in primary visual cortex neurons is illustrated in Fig. 10A. This is a very simplified illustration, but it demonstrates the essential concept. When a vertically oriented stimulus moves from left to right, the signals from the nondirection-selective inputs arrive simultaneously at the summation stage (as a consequence of the delay) and thus produce a relatively large response. On the other hand, when the stimulus moves from right to left, the signals arrive at different times and thus produce a weaker response. As illustrated in Fig. 10B, direction selectivity for motion parallel to the spatial orientation of the receptive field can be obtained in a similar fashion by rotating the preferred spatial orientation of the two nondirection-selective inputs. The solid curves in Fig. 8 show the predictions of the *standard model* with the spatial orientation of the two components simply rotated by 90 deg.

Cortical neurons that show direction selectivity for both perpendicular and parallel motion could potentially be produced by slightly more complex configurations of spatial and temporal offsets. For example, as illustrated by the "mixed case" in Fig. 10C, time delays *between* the rows (of center/surround units) can produce direction selectivity for perpendicular motion, and time delays *within* the rows (of center/surround units) can produce direction selectivity for parallel motion. As described in the Methods section, we model the mixed case by generalizing the *single axis* linear spatio-temporal filter [see eqn. (1)] proposed by Watson and Ahumada (1985) to form a *double axis* linear spatio-temporal filter [see eqn. (2)]. The solid curves in Fig. 9 show the predictions of a model that allows two axes of direction selectivity.

The *standard model*, generalized to include *double axis* linear spatio-temporal filters, predicts that there should be modest asymmetries in the orientation tuning functions for opposite directions of motion, measured with drifting sine-wave gratings. As illustrated in Fig. 7D, the values of parallel direction selectivity range from approximately 0 to 0.6, with a median value of approximately 0.3. The generalized *standard model* predicts that a parallel direction selectivity of 0.3 should produce an asymmetrical shift in the orientation tuning of only a few degrees: approximately 3 deg for each direction of motion. In other words, modest orientation-tuning asymmetries are an expected side effect of the linear-quadrature models for parallel motion direction selectivity.

The orientation-tuning asymmetries predicted by the generalized *standard model* are quite small. Nonetheless, we attempted to determine whether they could be detected in the orientation tuning functions we measured for each neuron prior to presenting the spots or plaids (see Methods). To do this, we fitted the orientation responses from each cell with a pair of asymmetric Gaussian functions, where the standard deviations on the two sides of the peak (for each direction of motion) were free to vary, and the separation in the peaks for the opposite directions of motion were also free to vary (a total of 8 free parameters). We found that some cells did show small asymmetries, but they did not appear to be systematically related to the degree of parallel motion direction selectivity. In order to detect the small orientation asymmetries

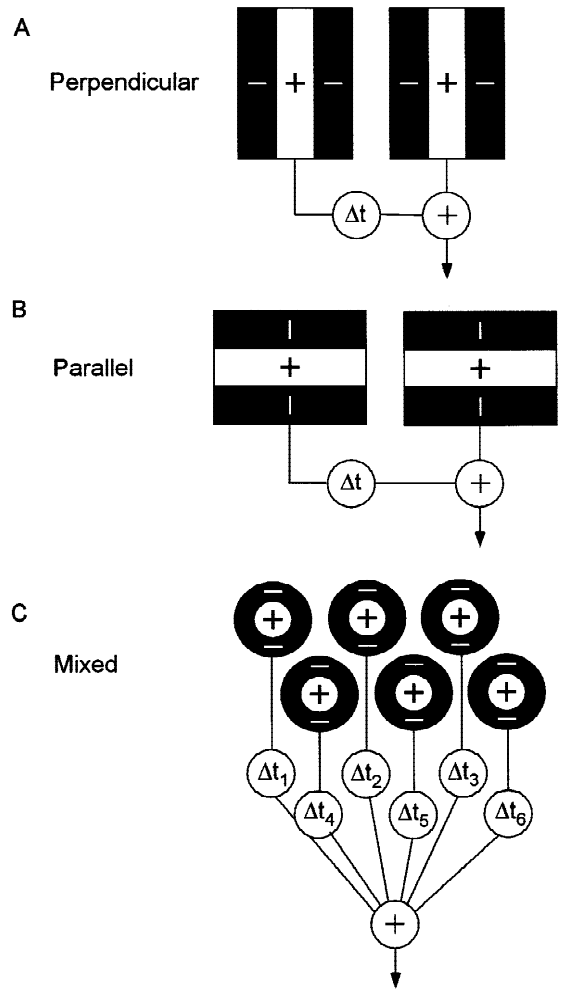

Fig. 10. Schematic diagrams that illustrate plausible simple methods for producing *single-axis* and *double-axis* direction-selective mechanisms. (A) Traditional *single-axis* model of direction selectivity in primary visual cortex. Spatial offsets (or spatial phase differences) are combined with temporal offsets (or temporal phase differences) to produce direction selectivity for motion perpendicular to the spatial orientation of the receptive field. (B) Nontraditional *single-axis* model of direction selectivity. Spatial offsets (or spatial phase differences) are combined with temporal offsets (or temporal phase differences) to produce direction selectivity for motion parallel to the spatial orientation of the receptive field. (C) Nontraditional *double-axis* model of direction selectivity. Various spatial offsets (or spatial phase differences) are combined with various temporal offsets (or temporal phase differences) to produce direction selectivity for both motion perpendicular to and motion parallel to the spatial orientation of the receptive field.

predicted by the generalized *standard model*, it would probably be necessary to measure the orientation tuning functions with smaller orientation increments (e.g. every 1 or 2 deg).

Others have measured the direction-selective responses of primary visual cortex neurons with moving plaid and checkerboard patterns (De Valois et al., 1979; Movshon et al., 1985), but they have not reported direction selectivity for motion parallel to the spatial orientation of the receptive field. The explanation seems to be that the spatial components in the previous studies were optimized for some direction of motion other than parallel motion, and hence did not produce sufficiently large responses to measure direction selectivity for parallel motion. For example, the plaid patterns used by Movshon et al. (1985) in V1 are illustrated in Fig. 11A. The grating patterns indicate the two sine-wave components that are summed to create the plaid pattern; the arrows on each component indicate the motion direction of the component and the other arrows indicate the motion for the whole pattern. For the 90 deg plaid, almost no response is produced by either the parallel or the perpendicular motion because the orientations of the components are 45 deg from the preferred orientation of the neuron. (Note that the average half-bandwidth of V1 neurons is 20 deg.) To obtain a large response, the motion direction must be such that one of the components falls within the orientation bandwidth of the neuron, and thus the motion of that component will be approximately perpendicular to the cell's preferred spatial orientation. The stimuli used in the present study are illustrated in Fig. 11B. Here, large responses are produced for both parallel and perpendicular motion because the two spatial components are always well within the orientation bandwidth of the neuron.

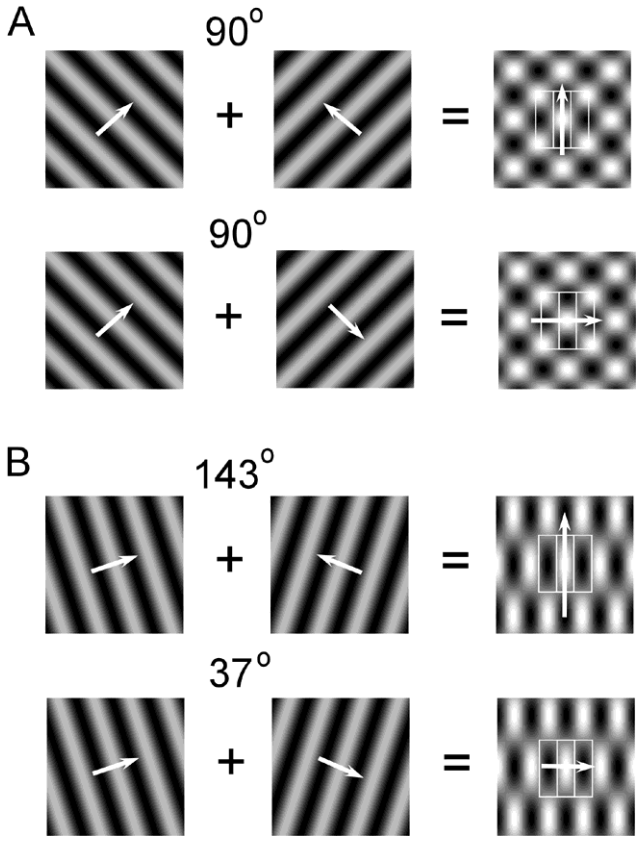

Fig. 11. Illustration of the differences in the plaid stimuli used by Movshon et al. (1985) and the plaid stimuli used in the present study. These differences may explain why direction selectivity for parallel motion has not been reported previously for plaid or checkerboard patterns. The grating patterns indicate the two drifting sine-wave components that are summed to create the plaid pattern; arrows on the gratings indicate the direction of motion of each component. The numbers indicate the angles between the drifting components. The arrows on the plaid indicate the direction of motion of the plaid. (A) Stimuli used by Movshon et al. (1985). For the 90-deg plaid, almost no response is produced by either the parallel or the perpendicular motion because the orientations of the components are 45 deg from the preferred orientation of the neuron. (B) Stimuli used in the present study. Strong responses are produced for both parallel and perpendicular motion because the two spatial components are always well within the orientation bandwidth of the neuron.

At first thought, the "parallel motion direction selective neurons" that we have found in V1 might seem similar to the "Type II neurons" that Albright (1984) found in the middle temporal area (MT). Type II neurons show direction selectivity for drifting bars and spots that move approximately parallel to the preferred spatial orientation, as measured with stationary bars. However, Albright (1984) did not find Type II neurons in V1. Furthermore, the parallel motion direction-selective neurons in V1 show direction selectivity for spots that move perpendicular to optimal gratings and bars that are either stationary or drifting. In other words, Type II neurons behave differently when measured with drifting as opposed to stationary bars or gratings, whereas the V1 neurons behave similarly. Finally, given that Rodman and Albright (1989) have demonstrated that the Type II neurons (in area MT) correspond to the pattern direction-selective neurons (also in area MT; Movshon et al., 1985), it is worth noting that Movshon et al. did not find pattern direction-selective neurons in area V1 (see also De Valois et al., 1979). Thus, it seems reasonable to conclude that the area MT Type II neurons do not correspond to the parallel motion direction-selective neurons that we have found in the primary visual cortex. However, it is possible that feedback from MT neurons could contribute to the parallel direction selectivity seen in V1 (Maunsell & van Essen, 1983; Rockland & Van Hoesen, 1994).

Cortical neurons are known to be quite selective: Most individual neurons are simultaneously selective along the dimensions of position, orientation, spatial frequency, temporal frequency, and the direction of motion perpendicular to the preferred spatial orientation (see references cited earlier for the *standard model*). Here, we have shown that many cortical neurons are also selective for the direction of motion parallel to the preferred spatial orientation. This fact implies that cortical neurons are even more selective than was previously thought; that is, the domain of spatio-temporal stimulation to which the typical cortical neuron responds is even more restricted. The degree of direction selectivity for parallel motion is, on average, less than for perpendicular motion, but it is still substantial, and may have important implications for neural computation and perception.

Temporal-frequency tuning and motion streaks

Motion streak signals are the result of temporal integration in the visual system. Simulations of V1 neuron responses, based upon the *standard model* (Geisler, 1999), have shown that motion streak signals should exist in the primary visual cortex because of the substantial temporal integration that occurs within the early stages of the visual system. When those simulations were performed, the temporal integration interval for motion that is perpendicular to the orientation of the receptive field of V1 neurons was well established (e.g. Movshon et al, 1978*b*; Foster et al., 1985; Hamilton

et al., 1989; Hawken et al., 1996); however, the integration interval for motion parallel to the orientation of the receptive field was unknown. Due to this lack of information, Geisler assumed that the temporal integration interval for parallel motion was equivalent to the temporal integration interval for perpendicular motion. As shown in Figs. 6–9, the shape of the temporal-frequency tuning function, and hence the temporal integration interval, is very similar for parallel and perpendicular motion, and thus it substantiates the earlier simulations. Further, this fact indicates that motion streak signals should be present in the responses of V1 neurons under a wide range of circumstances. The temporal-frequency tuning for parallel motion provides an additional estimate, and perhaps a more reliable estimate, of the critical speed at which motion streaks should occur.

It is worth noting that under scotopic conditions, when visual sensitivity is based upon the responses of the rods, the temporal integration interval increases. The integration time for a rod is approximately three times longer than the integration time for a cone (e.g. see Walraven et al., 1990). This implies that under scotopic conditions, when other cues for the direction of object motion are likely to be diminished, motion streak signals may play an even more important role in the perception of motion direction.

Motion streak signals in V1

Taken as a whole, the neurophysiological measurements reported here, along with the psychophysical measurements, and simulations, reported elsewhere (Geisler, 1999), strongly suggest that when an image feature moves with sufficient speed it should create a "local orientation maximum," as illustrated in Fig. 1B. This local orientation maximum could potentially be used to signal the direction of the feature's motion. Further, because the critical speed for producing a spatial motion streak is relatively low, such signals should be present in V1 under a wide range of natural viewing conditions.

It is reasonable to consider how subsequent brain mechanisms might extract motion direction from these motion streak signals in V1. This is a nontrivial problem because motion streaks provide ambiguous information about motion direction. Specifically, a local orientation maximum (see Fig. 1B) could be the result of (1) an image feature that is moving parallel to the preferred orientation at the maximum, or (2) simply a contour that is aligned parallel to the preferred orientation at the maximum. Further, even if the local orientation maximum is the result of an image feature moving along the orientation at the maximum, the direction of motion along that orientation is uncertain (i.e. it could be moving in either of the opposite directions that is parallel to the preferred orientation).

One possible resolution to the ambiguities inherent in the local orientation maximum could be obtained by combining that signal with the local average direction-selective response. Specifically, the direction-selective response of the local population of V1 neurons could be used to determine the sign of the motion direction (1, −1, or 0). The peak of the local orientation maximum could then be multiplied by this sign. (Note that a sign of 0 corresponds to no movement.) We have shown that once the critical speed is exceeded, this simple mechanism correctly determines the motion direction of moving features within complex natural images (see Fig. 3 in Geisler, 1999).

A second possible resolution to the ambiguities inherent in the local orientation maximum could be obtained by combining the output of the neurons that are direction selective for parallel motion, at a subsequent stage. Specifically, the visual system could construct motion-opponent mechanisms (like those proposed by Adelson & Bergen,1985; and van Santen & Sperling, 1985), from the neurons that are direction selective for parallel motion (such as the ones illustrated in Figs. 8 and 9). As illustrated in Fig. 12A, such motion-opponent mechanisms can be obtained by differencing the output of two neurons that are direction selective for parallel motion, with opposite preferred directions of motion. A population of such motion-opponent neurons could be used for measuring motion direction from motion streaks signals. Static features would produce no response. However, as illustrated in Fig. 12B, features moving above the critical speed will produce a local maximum in the population of opponent cells. This local maximum response will correspond to the direction of feature motion.

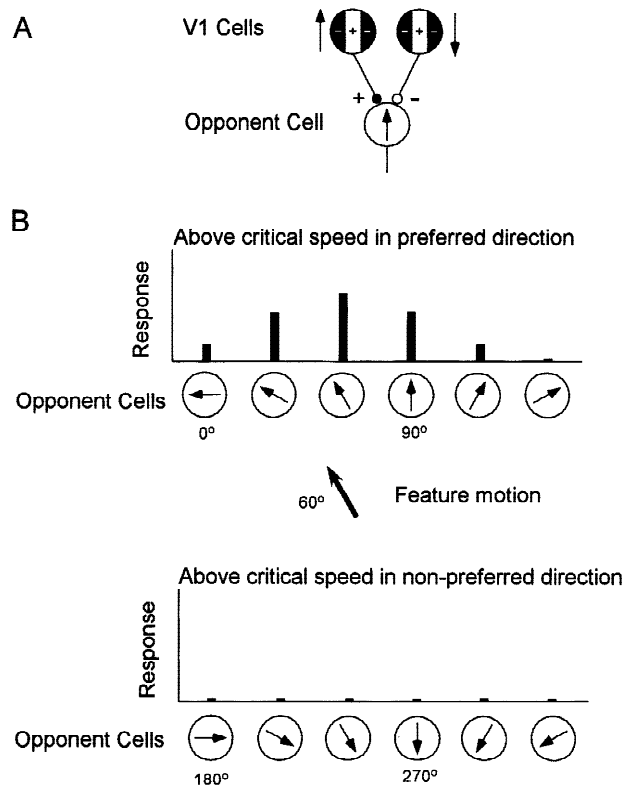

Fig. 12. Illustration of how parallel direction-selective neurons could be used to encode motion direction. (A) Hypothetical opponent cell created by combining parallel direction-selective cells with opposite preferences for motion direction. (B) Responses across a population of hypothetical opponent cells with different preferences for motion direction, to a feature moving in the direction indicated by the arrow. The population does not respond to static features. However, if the feature is moving above a critical speed, the peak in the distribution of activity corresponds to the direction of motion.

Glass patterns and motion streak mechanisms

Some recently reported psychophysical phenomena involving interactions between motion and spatial vision may provide further evidence for a motion streak mechanism. Ross et al. (2000) created dynamic displays where each display frame was a different random

sample of a *Glass pattern* (which consists of randomly positioned pairs of dots).†† Although such displays contain no coherent motion energy, the subjects reported a strong motion perception in the direction that corresponded to the spatial orientation of the dot pairs. It is plausible that such a *Glass pattern* could activate a motion streak mechanism. The oriented dot pairs could effectively provide spatial streak signals and the dynamic noise could provide motion signals. Together they could activate a motion streak mechanism that would signal motion parallel to the orientation of the dot pairs (Ross et al., 2000; Burr, 2000). Francis and Kim (1999) report what may be related phenomena in ambiguous three-frame apparent motion displays.

Motion direction signals

Motion streak mechanisms are just one of several possible mechanisms the brain uses to determine motion direction. For example, plaid patterns should not produce motion streak signals (see footnote **); however, the direction of motion of plaid patterns can be correctly perceived. Thus, the visual system must use some other cue (or cues) for determining the direction of motion for moving plaids. As noted in the Introduction, there are at least two possible mechanisms: (1) combining velocity components at two or more orientations, and (2) matching or tracking features over time. Furthermore, except under scotopic conditions (when the temporal integration interval is three times longer), motion streaks are unlikely to be an important source of motion direction at slower speeds, unless there exists a specialized (unexplored) population of cells with very long temporal integration times.

With these limitations in mind, the motion streak mechanisms could potentially be very important to the visual system because they are complementary to other mechanisms. As speed increases, estimates of velocity components, and the ability to track features, become less reliable, while estimates of the spatial orientation of motion streaks become more reliable. Similar to the way the visual system determines an object's depth and distance, the visual system undoubtedly utilizes every available source of information to determine an object's direction of motion.

References

Adelson, E.H. & Bergen, J.R. (1985). Spatio-temporal energy models for the perception of motion. *Journal of the Optical Society of America A* **2**, 284–299.

Adelson, E.H. & Movshon, J.A. (1982). Phenomenal coherence of moving visual patterns. *Nature* **300**, 523–525.

Albrecht, D.G. & Geisler, W.S. (1991). Motion selectivity and the contrast-response function of simple cells in the visual cortex. *Visual Neuroscience* **7**, 531–546.

Albrecht, D.G. & Geisler, W.S. (1994). Visual cortex neurons in monkey and cat: Contrast response nonlinearities and stimulus selectivity. In *Computational Vision Based on Neurobiology, Vol. 2054*, ed. Lawton, T., pp. 12–31. Bellingham, Washington: SPIE.

Albright, T.D. (1984). Direction and orientation selectivity of neurons in visual area MT of the macaque. *Journal of Neurophysiology* **52**, 1106–1130.

Barlow, H.B. & Levick, W.R. (1965). The mechanism of directionally selective units in rabbit's retina. *Journal of Physiology* **178**, 477–504.

Burr, D. (2000). Are "speed lines" used in human visual motion? *Current Biology* **10**, R440–R443.

††A Glass pattern is an image consisting of a large number of randomly placed elements, where each element is a pair of dots. Although the elements are located randomly, the orientation of the elements may be the same or may vary systematically in some fashion across the image.

Carandini, M., Heeger, D.J. & Movshon, J.A. (1999). Linearity and gain control in V1 simple cells. In *Cerebral Cortex, Vol. 13: Models of Cortical Circuits*, ed. Ulinski, P.S., Jones, E.G. & Peters, A., pp. 401–426. New York: Kluwer Academic/Plenum Publishers.

Cavanaugh, P. (1992). Attention-based motion perception. *Science* **257**, 1563–1565.

DeAngelis, G.C., Ohzawa, I. & Freeman, R.D. (1993). Spatio-temporal organization of simple-cell receptive fields in the cat's striate cortex. II. Linearity of temporal and spatial summation. *Journal of Neurophysiology* **69**, 1118–1135.

DeAngelis, G.C., Freeman, R.D. & Ohzawa, I. (1994). Length and width tuning of neurons in the cat's primary visual cortex. *Journal of Neurophysiology* **71**, 347–374.

Derrington, A. (2000). Seeing motion. In *Seeing*, ed. De Valois, K.K., pp. 259–309. San Diego, California: Academic Press.

Derrington, A. & Suero, M. (1991). Motion of complex patterns is computed from the perceived motions of their components. *Vision Research* **31**, 139–149.

De Valois, K.K., De Valois, R.L. & Yund, W.E. (1979). Responses of striate cortex cells to grating and checkerboard patterns. *Journal of Physiology* **291**, 483–505.

De Valois, R.L., Albrecht, D.G. & Thorell, L.G. (1982*a*). Spatial frequency selectivity of cells in macaque visual cortex. *Vision Research* **22**, 545–559.

De Valois, R.L., Yund, E.W. & Hepler, N. (1982*b*). The orientation and direction selectivity of cells in macaque visual cortex. *Vision Research* **22**, 531–544.

De Valois, R.L., Thorell, L.G. & Albrecht, D.G. (1985). Periodicity of striate-cortex-cell receptive fields. *Journal of the Optical Society of America A* **2**, 1115–1123.

Emerson, R.C., Bergen, J.R. & Adelson, E.H. (1992). Directionally selective complex cells and the computation of motion energy in cat visual cortex. *Vision Research* **32**, 203–218.

Foster, K.H., Gaska, J.P., Nagler, M. & Pollen, D.A. (1985). Spatial and temporal frequency selectivity of neurons in visual cortical areas V1 and V2 of the macaque monkey. *Journal of Physiology* (London) **365**, 331–363.

Francis, G. & Kim, H. (1999). Motion parallel to line orientation: Disambiguation of motion percepts. *Perception* **28**(10), 1243–1255.

Gardner, J.L., Anzai, A., Ohzawa, I. & Freeman, R.D. (1999). Linear and nonlinear contributions to orientation tuning of simple cells in the cat's striate cortex. *Visual Neuroscience* **16**, 1115–1121.

Geisler, W.S. (1999). Motion streaks provide a spatial code for motion direction. *Nature* **400**, 65–69.

Geisler, W.S. & Albrecht, D.G. (1997). Visual cortex neurons in monkeys and cats: Detection, discrimination, and identification. *Visual Neuroscience* **14**, 897–919.

Geisler, W.S. & Albrecht, D.G. (2000). Spatial Vision. In *Seeing* (2nd edition), De Valois, K.K., pp. 79–128. New York: Academic Press.

Hamilton D.B., Albrecht, D.G. & Geisler, W.S. (1989). Visual cortical receptive fields in monkey and cat: Spatial and temporal phase transfer function. *Vision Research* **29**, 1285–1308.

Hawken, M.J., Shapley, R.M. & Grosof, D.H. (1996). Temporal frequency selectivity in monkey lateral geniculate nucleus and striate cortex. *Visual Neuroscience* **13**, 477–492.

Heeger, D.J. (1991). Nonlinear model of neural responses in cat visual cortex. In *Computational Models of Visual Perception*, ed. Landy, M.S. & Movshon, J.A., pp. 119–133. Cambridge, Massachusetts: The MIT press.

Heeger, D.J. (1992*a*). Half-squaring in responses of cat striate cells. *Visual Neuroscience* **9**, 427–443.

Heeger, D.J. (1992*b*). Normalization of cell responses in cat striate cortex. *Visual Neuroscience* **9**, 191–197.

Hubel, D.H. & Wiesel, T.N. (1962). Receptive fields, binocular interaction, and functional architecture in the cat's visual cortex. *Journal of Physiology* (London) **160**, 106–154.

Hubel, D.H. & Wiesel, T.N. (1968). Receptive fields and functional architecture of monkey striate cortex. *Journal of Physiology* (London) **195**, 215–243.

Marr, D. & Ullman, S. (1981). Direction selectivity and its use in early visual processing. *Proceedings of the Royal Society B* (London) **212**, 151–180.

Maunsell, J.H. & van Essen, D.C. (1983). The connections of the middle temporal visual area (MT) and their relationship to a cortical hierarchy in the macaque monkey. *Journal of Neuroscience* **3**, 2563–2586.

Metha, A.B., Crane, A.M., Rylander, H.G., Thomsen, S.L. & Albrecht, D.G. Maintaining the cornea and the general physiological environment in visual neurophysiology experiments. *Journal of Neuroscience Methods* (in press).

Movshon, J., Adelson, E.H., Martin, S.G. & Newsome, W.T. (1985). The analysis of moving visual patterns. In *Pattern Recognition Mechanisms,* ed. Chagras, C., Gatass, R. & Gross, C., pp. 117–151. New York: Springer Verlag.

Movshon, J.A., Thompson, I. & Tolhurst, D. (1978*a*). Spatial summation in the receptive fields of simple cells in the cat's striate cortex. *Journal of Physiology* (London) **283**, 53–57.

Movshon, J.A., Thompson, I.D. & Tolhurst, D.J. (1978*b*). Spatial and temporal contrast sensitivity of neurones in area 17 and 18 of cat's visual cortex. *Journal of Physiology* **283**, 101–120.

Palmer, L.A., Jones, J.P. & Stepnoski, R.A. (1991). Striate receptive fields as linear filters: Characterization in two dimensions of space. In *Vision and Visual Dysfunction, Vol. 4, The Neural Basis of Visual Function,* ed. Leventhal, A.C., pp. 246–260. Boca Raton, Florida: CRC Press, Inc.

Reichardt, W. (1961). Autocorrelation, a principle for the evaluation of sensory information by the central nervous system. In *Sensory Communication,* ed. Rosenblith, W.A., pp. 303–317. New York: Wiley.

Robson, J.G. (1975). Receptive fields: Neural representation of the spatial and intensive attributes of the visual image. In *Handbook of Perception, Vol. 5,* ed. Carterette, E.C. & Friedman, M.P., pp. 81–116. New York: Academic Press.

Rockland, K.S. & Van Hoesen, G.W. (1994). Direct temporal-occipital feedback connections to striate cortex (V1) in the macaque monkey. *Cerebral Cortex* **4**, 300–313.

Rodman, H.R. & Albright, T.D. (1989). Single-unit analysis of pattern-motion selective properties in the middle temporal visual area (MT). *Experimental Brain Research* **75**, 53–64.

Ross, J., Badcock, D.R. & Hayes, A. (2000). Coherent global motion in the absence of coherent velocity signals. *Current Biology* **10**, 679–682.

Shapley, R. & Lennie, P. (1985). Spatial frequency analysis in the visual system. *Annual Review of Neuroscience* **8**, 547–583.

Simoncelli, E.P. & Heeger, D.J. (1998). A model of neuronal responses in visual area MT. *Vision Research* **38**, 743–761.

Smith, A.T. & Snowden, R.J. (eds.) (1994). *Visual Detection of Motion*. London: Academic Press.

Stone, L.S., Watson, A.B. & Mulligan, J.B. (1990). Effect of contrast on the perceived direction of a moving plaid. *Vision Research* **30**, 1049–1067.

van Santen, J.P.H. & Sperling, G. (1985). Elaborated Reichardt detectors. *Journal of the Optical Society of America A* **2**, 300–321.

Walraven, J., Enroth-Cugell, C., Hood, D.C., MacLeod, D.I.A. & Schnapf, J.L. (1990). The control of visual sensitivity: Receptoral and postreceptoral processes. In *Visual Perception: The Neurophysiological Foundations,* ed. Spillman, L. & Werner, J.S., pp. 53–101. San Diego, California: Academic Press.

Watson, A.B. & Ahumada, A.J. (1985). Model of human visual-motion sensing. *Journal of the Optical Society of America A* **2**, 322–342.